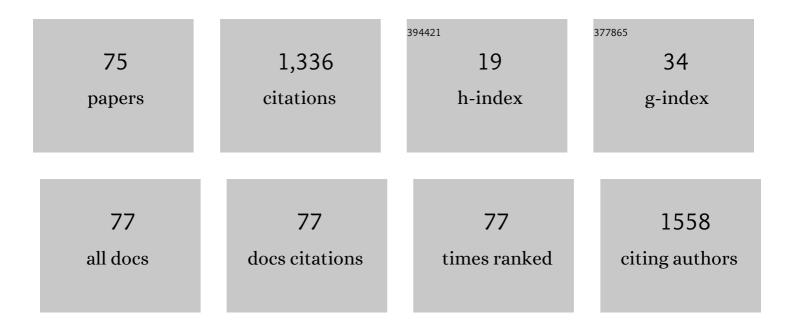
List of Publications by Year in descending order

Source: https://exaly.com/author-pdf/4501097/publications.pdf Version: 2024-02-01



#	Article	IF	CITATIONS
1	Optimized energy-storage performance in Mn-doped Na0.5Bi0.5TiO3-Sr0.7Bi0.2TiO3 lead-free dielectric thin films. Applied Surface Science, 2022, 571, 151274.	6.1	24
2	Porphyrin-based covalent triazine framework and its carbonized derivative as catalyst scaffold of Au and Ag nanoparticles for 4-nitrophenol reduction. Microporous and Mesoporous Materials, 2022, 330, 111611.	4.4	11
3	A slush-like polar structure for high energy storage performance in a Sr _{0.7} Bi _{0.2} TiO ₃ lead-free relaxor ferroelectric thin film. Journal of Materials Chemistry A, 2022, 10, 7357-7365.	10.3	20
4	Enhanced electrical properties of the polymorphic phase boundary on the tetragonal side in K0.48Na0.52NbO3-based lead-free piezoelectric ceramics. Ceramics International, 2022, 48, 17246-17252.	4.8	3
5	Orientation dependent intrinsic and extrinsic contributions to the piezoelectric response in lead-free (Na0.5K0.5)NbO3 based films. Journal of Alloys and Compounds, 2022, 906, 164346.	5.5	2
6	Enhanced strains by flexible nanoscale domain structure in BNKT-SBT relaxor ferroelectrics. Journal of Materials Chemistry C, 2022, 10, 9628-9635.	5.5	8
7	Enhanced large field-induced strain and energy storage properties of Sr0.6La0.2Ba0.1TiO3-modified Bi0.5Na0.5TiO3 relaxor ceramics. Journal of Materials Science: Materials in Electronics, 2022, 33, 15779-15790.	2.2	5
8	Synthesis of carbazole-based polymer derived N-enriched porous carbon for dyes sorption. Polymer Bulletin, 2021, 78, 3311-3325.	3.3	4
9	The formation process of aluminum hydroxide in calcium sulfoaluminate pastes. Chemical Papers, 2021, 75, 909-920.	2.2	2
10	Robust perfluorinated porous organic networks: Succinct synthetic strategy and application in chlorofluorocarbons adsorption. Nano Research, 2021, 14, 3282-3287.	10.4	9
11	High strain response and low hysteresis in BaZrO3-modified KNN-based lead-free relaxor ceramics. Journal of Materials Science: Materials in Electronics, 2021, 32, 16715-16725.	2.2	2
12	Electronic structure, morphology-controlled synthesis, and luminescence properties of YF3: Eu3+. Journal of Sol-Gel Science and Technology, 2021, 98, 497-507.	2.4	3
13	Large strain and low hysteresis in (1-x)Bi0.5(Na0.75K0.25)0.5TiO3-xSrTiO3 lead-free piezoceramics. Materials Research Express, 2021, 8, 056303.	1.6	2
14	Enhanced Electrostrictive Coefficient and Suppressive Hysteresis in Lead-Free Ba(1â^'x)SrxTiO3 Piezoelectric Ceramics with High Strain. Crystals, 2021, 11, 555.	2.2	6
15	Grain size engineering and growth mechanism in hydrothermal synthesis of Bi0.5Na0.5TiO3 thin films on Nb-doped SrTiO3 substrates. Journal of Sol-Gel Science and Technology, 2021, 99, 366-375.	2.4	7
16	Enhanced strains of Nb-doped BNKT-4ST piezoelectric ceramics via phase boundary and domain design. Ceramics International, 2021, 47, 24207-24217.	4.8	17
17	Ferroelectric–relaxor phase evolution and enhanced electromechanical strain response in LaAlO3-modified Bi0.5Na0.5TiO3–Bi0.5K0.5TiO3 lead-free ceramics. Journal of Materials Science: Materials in Electronics, 2021, 32, 28436-28446.	2.2	4
18	Heteroepitaxial Growth of 1T MoS 2 Nanosheets on SnO 2 with Synergetic Improvement on Photocatalytic Activity. Crystal Research and Technology, 2021, 56, 2000091.	1.3	4

#	Article	IF	CITATIONS
19	Large strain with low hysteresis in Sn-modified Bi0.5(Na0.75K0.25)0.5TiO3 lead-free piezoceramics. Journal of Materials Science, 2020, 55, 1388-1398.	3.7	19
20	Easy-to-use model to reveal the nature of octahedral rotation transformations in perovskites. Ceramics International, 2020, 46, 4477-4483.	4.8	2
21	Effects of sulfur substitution for oxygen on the thermoelectric properties of Bi2O2Se. Journal of the European Ceramic Society, 2020, 40, 5543-5548.	5.7	21
22	Realizing white emission in Sc2(MoO4)3:Eu3+/Dy3+/Ce3+ phosphors through computation and experiment. Journal of Solid State Chemistry, 2020, 290, 121592.	2.9	11
23	Elucidating the electronic structures and photoluminescence properties of single-phase ScF3:Dy3+, Eu3+, Ce3+ phosphors for LEDs. Journal of Sol-Gel Science and Technology, 2020, 96, 753-762.	2.4	3
24	Improved strain and low hysteresis in (0.9-x)BaTiO3-xCaTiO3-0.1Ba(Zr0.7Sn0.3)O3 lead-free relaxor ferroelectrics. Ceramics International, 2020, 46, 24231-24237.	4.8	4
25	<i>De novo</i> fabrication of multi-heteroatom-doped carbonaceous materials <i>via</i> an <i>in situ</i> doping strategy. Journal of Materials Chemistry A, 2020, 8, 4740-4746.	10.3	11
26	Evolution of mineral phases and microstructure of high efficiency Si–Ca–K–Mg fertilizer prepared by water-insoluble K-feldspar. Journal of Sol-Gel Science and Technology, 2020, 94, 3-10.	2.4	14
27	Fabrication of TiO2 nanofibers/MXene Ti3C2 nanocomposites for photocatalytic H2 evolution by electrostatic self-assembly. Applied Surface Science, 2019, 496, 143647.	6.1	131
28	Microwave hydrothermal synthesis, annealing and luminescence properties of BaWO4:3%Eu3+ microcrystals. Journal of Materials Science: Materials in Electronics, 2019, 30, 14190-14199.	2.2	3
29	Large strain response and fatigue-resistant behavior of lead-free (1-x)(Bi _{0.5} Na _{0.5})TiO ₃ - <i>x</i> SrTiO ₃ ceramics at a relatively low driving field. Materials Research Express, 2019, 6, 115218.	1.6	3
30	Nitrogen-rich hierarchical porous carbon supported Ag nanoparticles for efficient nitrophenol reduction. Microporous and Mesoporous Materials, 2019, 290, 109672.	4.4	16
31	Co3O4 nanocrystals grown on graphene nanosheets for high-performance supercapacitor with excellent rate capability. Journal of Sol-Gel Science and Technology, 2019, 89, 634-640.	2.4	3
32	Rapid synthesis of Ni(OH) ₂ /graphene nanosheets and NiO@Ni(OH) ₂ /graphene nanosheets for supercapacitor applications. New Journal of Chemistry, 2019, 43, 3091-3098.	2.8	30
33	TEM study of incommensurate superstructure in Pb1â^'0.5xNbx((Zr0.52Sn0.48)0.955Ti0.045)1â^'xO3 ceramics with 0–1 switching characteristic strain and high energy storage density. Journal of Materials Science: Materials in Electronics, 2019, 30, 12375-12381.	2.2	4
34	Giant strain response with low hysteresis in potassium sodium niobate based lead-free ceramics. Ceramics International, 2019, 45, 14675-14683.	4.8	10
35	Regulated morphology of ScF3: Eu3+, Bi3+ microcrystals: Microwave-assisted hydrothermal synthesis, structure and luminescence properties. Journal of Solid State Chemistry, 2019, 269, 447-453.	2.9	6
36	Erratum to "Nanoscale origins of small hysteresis and remnant strain in Bi0.5Na0.5TiO3-based lead-free ceramics―[Journal of the European Ceramic Society 37/11 (2017) 3483–3491]. Journal of the European Ceramic Society, 2018, 38, 359.	5.7	0

#	Article	IF	CITATIONS
37	A nanoscale porous glucose-based polymer for gas adsorption and drug delivery. New Journal of Chemistry, 2018, 42, 15692-15697.	2.8	3
38	Impact of Ni dopant on structure and electrical properties of PMN-0.1PT ceramics. Journal of Materials Science: Materials in Electronics, 2017, 28, 7525-7531.	2.2	7
39	Hypercrosslinked conjugated microporous polymers for carbon capture and energy storage. New Journal of Chemistry, 2017, 41, 3915-3919.	2.8	23
40	Nanoscale origins of small hysteresis and remnant strain in Bi 0.5 Na 0.5 TiO 3 -based lead-free ceramics. Journal of the European Ceramic Society, 2017, 37, 3483-3491.	5.7	35
41	Porphyrinâ€based covalent triazine frameworks: Porosity, adsorption performance, and drug delivery. Journal of Polymer Science Part A, 2017, 55, 2594-2600.	2.3	50
42	Enhanced energy storage properties of BiAlO3 modified Bi0.5Na0.5TiO3–Bi0.5K0.5TiO3 lead-free antiferroelectric ceramics. Ceramics International, 2017, 43, 7653-7659.	4.8	123
43	Preparation and electrical properties of Pb(1–1.5x)Lax(Zr0.66Sn0.25Ti0.09)O3 ceramics. Journal of Materials Science: Materials in Electronics, 2017, 28, 15953-15958.	2.2	1
44	Enhanced photoluminescence property of KLa1â^'xEux(MoO4)2 with concentration gradient. Journal of Materials Science: Materials in Electronics, 2017, 28, 4941-4945.	2.2	0
45	Phase transition and huge field-induced strain of BaZrO3 modified (Bi0.5Na0.5)0.94Ba0.06TiO3 ceramics. Journal of Materials Science: Materials in Electronics, 2017, 28, 14664-14671.	2.2	2
46	Huge strain and energy storage density of A-site La3+ donor doped (Bi0.5Na0.5)0.94Ba0.06TiO3 ceramics. Ceramics International, 2017, 43, 106-110.	4.8	64
47	Morphology and photoluminescent properties of KLa(MoO4)2 (doped with Eu3+) synthesized by a molten salt method. Journal of Materials Science: Materials in Electronics, 2016, 27, 10473-10478.	2.2	5
48	Morphology and photoluminescence properties of NaNd(MoO4)2 synthesized by a molten salt method. Journal of Materials Science: Materials in Electronics, 2016, 27, 5735-5740.	2.2	2
49	Enhanced energy storage properties of lead-free (1â^'x)Bi0.5Na0.5TiO3–xSrTiO3 antiferroelectric ceramics by two-step sintering method. Journal of Materials Science: Materials in Electronics, 2016, 27, 12479-12484.	2.2	27
50	Investigation of Multiply Twins in Mn _{2.02} Co _{0.98} O ₄ Ceramic by Means of Transmission Electron Microscopy. Journal of the American Ceramic Society, 2016, 99, 3458-3466.	3.8	3
51	Multiple morphologies of YF 3 : Eu 3+ microcrystals: Microwave hydrothemal synthesis, growth mechanism and luminescence properties. Ceramics International, 2016, 42, 1513-1520.	4.8	16
52	Citric sol–gel synthesis and luminescence characteristics of Ca1â^'y Sr y La2â^'x Eu x ZnO5 phosphors. Journal of Materials Science: Materials in Electronics, 2015, 26, 5618-5624.	2.2	1
53	Molten salt synthesis and tunable photoluminescent properties of Eu3+–Tb3+ doped NaY(MoO4)2 microcrystals. Journal of Materials Science: Materials in Electronics, 2015, 26, 2987-2994.	2.2	8
54	Citric acid-mediated microwave-assisted hydrothermal synthesis and luminescence property of NaSm(MoO4)2 submicro-crystals. Journal of Materials Science: Materials in Electronics, 2015, 26, 8595-8602.	2.2	4

#	Article	IF	CITATIONS
55	Preparation routes and electrical properties for Ni0.6Mn2.4O4 NTC ceramics. Journal of Materials Science: Materials in Electronics, 2015, 26, 7238-7243.	2.2	18
56	Microwave-assisted hydrothermal synthesis and photoluminescence property of NaSm(MoO4)2 octahedral crystals. Journal of Materials Science: Materials in Electronics, 2015, 26, 3926-3932.	2.2	3
57	Preparation and electrical properties of Ni0.6Mn2.4â^'Ti O4 NTC ceramics. Journal of Alloys and Compounds, 2015, 650, 931-935.	5.5	21
58	Facile synthesis of porous organic polymers bifunctionalized with azo and porphyrin groups. RSC Advances, 2015, 5, 98508-98513.	3.6	23
59	MICROWAVE-ASSISTED HYDROTHERMAL SYNTHESIS AND LUMINESCENCE PROPERTIES OF Eu ³⁺ -DOPED CdTe QUANTUM DOTS. Nano, 2014, 09, 1450044.	1.0	3
60	Enhanced energy-storage properties of SrTiO3 doped (Bi1/2Na1/2)TiO3–(Bi1/2K1/2)TiO3 lead-free antiferroelectric ceramics. Journal of Materials Science: Materials in Electronics, 2014, 25, 4632-4637.	2.2	50
61	Enhanced energy-storage properties of 0.89Bi 0.5 Na 0.5 TiO 3 –0.06BaTiO 3 –0.05K 0.5 Na 0.5 NbO 3 lead-free anti-ferroelectric ceramics by two-step sintering method. Materials Letters, 2014, 114, 107-110.	2.6	127
62	Using layer-by-layer assembly to fabricate NaLa(MoO4)2@CdTe core–shell microspheres with high fluorescence. Journal of Materials Science, 2014, 49, 4506-4512.	3.7	2
63	Growth of Bi1.5MgNb1.5O7 thin films on Pt/Ti/SiO2/Si substrates by RF magnetron sputtering. Journal of Materials Science: Materials in Electronics, 2014, 25, 1474-1479.	2.2	5
64	Microwave hydro/solvothermal synthesis of octahedron-like NaEu(MoO4)2 microarchitectures by EDTA-assisted and photoluminescence property. Journal of Materials Science: Materials in Electronics, 2014, 25, 2359-2365.	2.2	8
65	Highly uniform NaLa(MoO4)2:Eu3+ microspheres: microwave-assisted hydrothermal synthesis, growth mechanism and enhanced luminescent properties. Journal of Materials Science: Materials in Electronics, 2014, 25, 3109-3115.	2.2	13
66	Morphology and photoluminescence properties of KSm(MoO4)2 microcrystals by a molten salt method. Journal of Materials Science: Materials in Electronics, 2014, 25, 3608-3613.	2.2	6
67	Structure and dielectric properties of Nd substituted Bi1.5MgNb1.5O7 ceramics. Journal of Materials Science: Materials in Electronics, 2013, 24, 2785-2789.	2.2	11
68	Preparation and characterization of Ni0.6Mn2.4O4 NTC ceramics by solid-state coordination reaction. Journal of Materials Science: Materials in Electronics, 2013, 24, 5183-5188.	2.2	10
69	Sputtering pressure dependent composition and dielectric properties in Bi1.5MgNb1.5O7 thin films deposited at room temperature by RF magnetron sputtering. Journal of Materials Science: Materials in Electronics, 2013, 24, 5085-5090.	2.2	3
70	Morphology-controlled synthesis, characterization, and luminescence properties of KEu(MoO4)2 microcrystals. CrystEngComm, 2013, 15, 2761.	2.6	37
71	Morphology and Photoluminescence of Ba _{0.5} Sr _{0.5} MoO ₄ Powders by a Molten Salt Method. Journal of Nanomaterials, 2012, 2012, 1-6.	2.7	25
72	Seed layer-free electrodeposition and characterization of vertically aligned ZnO nanorod array film. Journal of Solid State Electrochemistry, 2010, 14, 63-70.	2.5	38

#	Article	IF	CITATIONS
73	Hydrothermal synthesis of monosized Bi0.5Na0.5TiO3 spherical particles under low alkaline solution concentration. Journal of Alloys and Compounds, 2009, 484, 801-805.	5.5	50
74	Synthesis and Photoluminescence of Assembly-Controlled ZnO Architectures by Aqueous Chemical Growth. Journal of Physical Chemistry C, 2009, 113, 1052-1059.	3.1	62
75	Structure and electric properties of (1â^'x)(Bi1/2Na1/2) TiO3-xBaTiO3 Systems. Journal Wuhan University of Technology, Materials Science Edition, 2007, 22, 315-319.	1.0	5